

EqCo: Equivalent Rules for Self-supervised Contrastive Learning

Benjin Zhu^{*1} Junqiang Huang^{*1} Zeming Li¹ Xiangyu Zhang¹ Jian Sun¹

Abstract

In this paper, we propose a method, named EqCo (**E**quivalent Rules for **C**ontrastive Learning), to make self-supervised learning irrelevant to the number of negative samples in InfoNCE-based contrastive learning frameworks. Inspired by the InfoMax principle, we point that the margin term in contrastive loss needs to be adaptively scaled according to the number of negative pairs in order to keep steady mutual information bound and gradient magnitude. EqCo bridges the performance gap among a wide range of negative sample sizes, so that we can use only a few negative pairs (e.g. 16 per query) to perform self-supervised contrastive training on large-scale vision datasets like ImageNet, while with almost no accuracy drop. This is quite a contrast to the widely used large batch training or memory bank mechanism in current practices. Equipped with EqCo, our simplified MoCo (SiMo) achieves comparable accuracy with MoCo v2 on ImageNet (linear evaluation protocol) while only involves 4 negative pairs per query instead of 65536, suggesting that large quantities of negative samples might not be a critical factor in InfoNCE loss.

1. Introduction

Self-supervised learning has recently received much attention in the field of visual representation learning (Hadsell et al., 2006; Dosovitskiy et al., 2014; Oord et al., 2018; Bachman et al., 2019; Hénaff et al., 2019; Wu et al., 2018; Tian et al., 2019; He et al., 2020; Misra & Maaten, 2020; Grill et al., 2020; Cao et al., 2020; Tian et al., 2020), as its potential to learn universal representations from unlabeled data. Among various self-supervised methods, one of the most promising research paths is *contrastive learning* (Oord et al., 2018), which has been demonstrated to achieve comparable or even better performances than supervised training for many downstream tasks such as image classification, object

detection, and semantic segmentation (Chen et al., 2020c; He et al., 2020; Chen et al., 2020a;b).

The core idea of contrastive learning is briefly summarized as follows: first, extracting a pair of embedding vectors ($\mathbf{q}(I), \mathbf{k}(I)$) (named *query* and *key* respectively) from the two augmented views of each instance I ; then, learning to maximize the similarity of each *positive pair* ($\mathbf{q}(I), \mathbf{k}(I)$) while pushing the *negative pairs* ($\mathbf{q}(I), \mathbf{k}(I')$) (i.e., query and key extracted from different instances accordingly) away from each other. To learn the representation, an *InfoNCE loss* (Oord et al., 2018; Wu et al., 2018) is conventionally employed in the following formulation (slightly modified with an additional *margin* term):

$$\mathcal{L}_{NCE} = \mathbb{E}_{\substack{\mathbf{q} \sim \mathcal{D}, \mathbf{k}_i \sim \mathcal{D}' \\ \mathbf{k}_0 \sim \mathcal{D}'(\mathbf{q})}} \left[-\log \frac{e^{(\mathbf{q}^\top \mathbf{k}_0 - m)/\tau}}{e^{(\mathbf{q}^\top \mathbf{k}_0 - m)/\tau} + \sum_{i=1}^K e^{\mathbf{q}^\top \mathbf{k}_i/\tau}} \right], \quad (1)$$

where \mathbf{q} and \mathbf{k}_i ($i = 0, \dots, K$) stand for the query and keys sampled from the two (augmented) data distributions \mathcal{D} and \mathcal{D}' respectively. Specifically, \mathbf{k}_0 is associated to the same instance as \mathbf{q} 's while other \mathbf{k}_i s not; hence we name \mathbf{k}_0 and \mathbf{k}_i ($i > 0$) *positive sample* and *negative samples* respectively in the remaining text, in which K is the number of negative samples (or pairs) for each query. The *temperature* τ and the *margin* m are hyper-parameters. In most previous works, m is trivially set to zero (e.g. Oord et al. (2018); He et al. (2020); Chen et al. (2020a); Tian et al. (2020)) or some handcraft values (e.g. Xie et al. (2020)). In the following text, we mainly study contrastive learning frameworks with InfoNCE loss as in Eq. 1 (or noted as *InfoNCE-based frameworks*) unless otherwise specified.¹

In *InfoNCE-based* contrastive learning research, it has been widely believed that enlarging the number of negative samples K boosts the performance (Hénaff et al., 2019; Tian et al., 2019; Bachman et al., 2019). For example, in MoCo (He et al., 2020) the ImageNet accuracy rises from 54.7% to 60.6% under linear classification protocol when K grows from 256 to 65536. Such observation further drives a line of

^{*}Equal contribution. ¹MEGVII Technology. Correspondence to: Xiangyu Zhang <zhangxiangyu@megvii.com>.

¹Recently, some self-supervised learning algorithms achieve new state-of-the-art results using different frameworks instead of conventional *InfoNCE* loss as in Eq. 1, e.g. *mean teacher* (in BYOL (Grill et al., 2020)) and *online clustering* (in SWAV (Caron et al., 2020b)). We will investigate them in the future.

studies how to effectively optimize under a number of negative pairs, such as *memory bank* methods (Wu et al., 2018; He et al., 2020) and large batch training (Chen et al., 2020a), either of which empirically reports superior performances when K becomes large. Analogously, in the field of *supervised metric learning* (Deng et al., 2019; Wang et al., 2018; Sun et al., 2020; Wang et al., 2020), loss in the similar form as Eq. 1 is often applied on a lot of negative pairs for hard negative mining. Besides, there are also a few theoretical studies supporting the viewpoint. For instance, Oord et al. (2018) points out that the mutual information between the positive pair tends to increase with the number of negative pairs K ; Wang & Isola (2020) finds that the negative pairs encourage features’ uniformity on the hypersphere; Chuang et al. (2020) suggests that large K leads to more precise estimation of the debiased contrastive loss; etc.

Despite the above empirical or theoretical evidence, however, recent researches imply it is still an open question whether large quantities of negative samples are crucial. **First**, unlike the metric learning mentioned above, in self-supervised learning, the negative terms k_i in Eq. 1 include both “true negative” (whose underlying class label is different from the query’s, similarly hereinafter) and “false negative” samples, since the actual ground truth label is not available. So, intuitively large K should not always be beneficial because the risk of false negative samples also increases (known as *class collision* problem). Arora et al. (2019) thus theoretically concludes that a large number of negative samples could not necessarily help. **Second**, some recent works have proven that by introducing new architectures (e.g., an *asymmetric* predictor network in BYOL (Grill et al., 2020; Richemond et al., 2020)), designing new loss functions (e.g., Caron et al. (2020a); Ermolov et al. (2020)) or adopting specially-designed optimization methods (e.g. *stop-gradient trick* in SimSiam (Chen & He, 2020)), state-of-the-art performance can still be obtained even *without* any explicit negative pairs. Although those methods *do not* exploit InfoNCE loss directly, they challenge the belief that self-supervised contrastive learning requires many negative pairs to obtain competitive performance in general.

Motivated by the success of frameworks free of negative samples such as BYOL, back to the *InfoNCE-based* approach, naturally we rise a question: **is a large K really essential in InfoNCE loss?** We propose to rethink the question from a different view: note that in Eq. 1, there are three hyper-parameters: the number of negative samples K , temperature τ , and margin m . In most of previous empirical studies (He et al., 2020; Chen et al., 2020a), only K is changed while τ and m are usually kept constant. *Do the optimal hyper-parameters of τ and m varies with K ?* If so, the performance gains observed from larger K s may be a *wrong* interpretation – merely brought by suboptimal hyper-parameters’ choices for small K s, rather than much

of an essential.

In the paper, we investigate the relationship among three hyper-parameters and suggest an *equivalent rule*:

$$m = \tau \log \frac{\alpha}{K},$$

where α is a constant. We find that if the margin m is adaptively adjusted based on the above rule, the performance of contrastive learning is *irrelevant* to the size of K , in a very large range (e.g. $K \geq 16$). For example, in MoCo framework, by introducing EqCo the performance gap between $K = 256$ and $K = 65536$ (the best configuration reported in (He et al., 2020)) *almost disappears* (from 6.1% decrease to 0.2%). We call this method “**E**quivalent Rules for **C**ontrastive learning” (*EqCo*). For completeness, as the other part of EqCo we point that adjusting the learning rate according to the conventional *linear scaling rule* satisfies the equivalence for different number of *queries* per batch.

Theoretically, following the *InfoMax principle* (Linsker, 1988) and the derivation in CPC (Oord et al., 2018), we prove that in *EqCo*, the lower bound of the mutual information keeps steady under various numbers of negative samples K . Moreover, from the back-propagation perspective, we further prove that in such configuration the upper bound of the gradient norm is also free of K ’s scale. The proposed equivalent rule implies that, by assigning $\alpha = K_0$, it can “mimic” the optimization behavior under K_0 negative samples even if the *physical* number of negatives $K \neq K_0$.

The “equivalent” methodology of *EqCo* is analogous to the well-known *linear scaling rule* (Krizhevsky, 2014; Goyal et al., 2017), which suggests scaling the learning rate proportional to the batch size if the loss satisfies with the linear averaged form: $L = \frac{1}{N} \sum_{i=1}^N f(x_i; \theta)$. However, *linear scaling rule* cannot be directly applied on InfoNCE loss (Eq. 1), which is partially because InfoNCE loss includes two batch sizes (number of *queries* and *keys* respectively) while linear scaling rule only involves one, in addition to the nonlinearity of the keys in InfoNCE loss. In the experiments of *SimCLR* (Chen et al., 2020a), learning rates under different batch sizes are adjusted with linear scaling rule, but the accuracy gap is still very large (57.5%@batch=256 vs. 64+%@batch=8192, 100 epochs training).

In InfoNCE-based contrastive learning frameworks, EqCo significantly reduces the demand for the size of negative pairs, making it possible to design simpler algorithms. We thus present *SiMo*, a simplified contrastive learning framework based on *MoCo v2* (Chen et al., 2020c). *SiMo* is elegant, efficient, free of large batch training and memory bank; moreover, it can achieve competitive performances among the state-of-the-arts even if the number of negative pairs is extremely small (e.g. 4), without bells and whistles.

The contributions of our paper are summarized as follows:

- We challenge the widely accepted belief that InfoNCE-based contrastive learning frameworks benefit *essentially* from large size of negative samples. Though more negative pairs are usually reported to derive better results in previous works, we interpret the phenomenon from a different view: it may be because the hyper-parameters in the loss are not set to the optimum according to different numbers of *keys* respectively.
- We propose EqCo, an equivalent rule to adaptively set hyper-parameters in the InfoNCE loss between small and large numbers of negative samples, which proves to bridge the performance gap.
- We present SiMo, a simple but strong alternative for contrastive learning based on InfoNCE loss. Thanks to EqCo, SiMo requires much fewer negative samples than the counterparts to achieve high performances.

2. EqCo: Equivalent Rules for Contrastive Learning

In this section we introduce *EqCo*. We mainly consider the circumstance of optimizing the *InfoNCE loss* (Eq. 1) with *SGD*. For each batch of training, there are two meanings of the concept “batch size”, i.e., the size of *negative samples/pairs* K per query, and the number of *queries* (or *positive pairs*) N per batch. Hence our equivalent rules accordingly consist of two parts, which will be introduced in the next subsections.

2.1. The Case of Negative Pairs

Our derivation is mainly inspired by the model of *Contrastive Predictive Coding (CPC)* (Oord et al., 2018), in which *InfoNCE loss* is interpreted as a mutual information estimator. We further extend the method so that it is applicable to InfoNCE loss with a *margin* term (Eq. 1), which is not considered in Oord et al. (2018).

Following the concept in Oord et al. (2018), given a *query* embedding \mathbf{q} (namely the *context* in Oord et al. (2018)) and suppose $(K + 1)$ random *key* embeddings $\mathbf{x} = \{\mathbf{x}_i\}_{i=0,\dots,K}$, where there exists exactly one entry (e.g., \mathbf{x}_i) sampled from the conditional distribution $P(\mathbf{x}_i|\mathbf{q})$ while others (e.g., \mathbf{x}_j) sampled from the “proposal” distribution $P(\mathbf{x}_j)$ independently. According to which entry corresponds to the conditional distribution, we therefore defines $(K + 1)$ *candidate* distributions for \mathbf{x} (denoted by $\{H_i\}_{i=0,\dots,K}$), where the probability density of \mathbf{x} under H_i is $P_{H_i}(\mathbf{x}) = P(\mathbf{x}_i|\mathbf{q}) \prod_{j \neq i} P(\mathbf{x}_j)$. So, given the observed data $X = \{\mathbf{k}_0, \dots, \mathbf{k}_K\}$ of \mathbf{x} , the probability where \mathbf{x} is sampled from H_0 rather than other candidates is thus de-

rived with Bayes theorem:

$$\begin{aligned} \Pr[\mathbf{x} \sim H_0|\mathbf{q}, X] &= \frac{P^+ P_{H_0}(X)}{P^+ P_{H_0}(X) + P^- \sum_{i=1}^K P_{H_i}(X)} \\ &= \frac{\frac{P^+}{P^-} \frac{P(\mathbf{k}_0|\mathbf{q})}{P(\mathbf{k}_0)}}{\frac{P^+}{P^-} \frac{P(\mathbf{k}_0|\mathbf{q})}{P(\mathbf{k}_0)} + \sum_{i=1}^K \frac{P(\mathbf{k}_i|\mathbf{q})}{P(\mathbf{k}_i)}}, \end{aligned} \quad (2)$$

where we denote P^+ and P^- as the *prior* probabilities of H_0 and $H_i (i > 0)$ respectively. We point that Eq. 2 introduces a *generalized form* to that in Oord et al. (2018) by taking the priors into account. Referring to the notations in Eq. 1, we suppose that H_0 is the ground truth distribution of \mathbf{x} (since \mathbf{k}_0 is the only positive sample). By modeling the density ratio $P(\mathbf{k}_i|\mathbf{q})/P(\mathbf{k}_i) \propto e^{\mathbf{q}^\top \mathbf{k}_i/\tau} (i = 0, \dots, K)$ and letting $P^+/P^- = e^{-m/\tau}$, the negative log-likelihood $\mathcal{L}_{opt} \triangleq \mathbb{E}_{\mathbf{q}, X} -\log \Pr[x \sim H_0|\mathbf{q}, X]$ can be regarded as the “optimal” target of \mathcal{L}_{NCE} .

Similar to the methodology of Oord et al. (2018), we explore the lower bound of \mathcal{L}_{opt} :

$$\begin{aligned} \mathcal{L}_{opt} &= \mathbb{E}_{\substack{\mathbf{q} \sim \mathcal{D}, \mathbf{k}_i \sim \mathcal{D}' \\ \mathbf{k}_0 \sim \mathcal{D}'(\mathbf{q})}} \log \left(1 + e^{m/\tau} \frac{P(\mathbf{k}_0)}{P(\mathbf{k}_0|\mathbf{q})} \sum_{i=1}^K \frac{P(\mathbf{k}_i|\mathbf{q})}{P(\mathbf{k}_i)} \right) \\ &\approx \mathbb{E}_{\substack{\mathbf{q} \sim \mathcal{D} \\ \mathbf{k}_0 \sim \mathcal{D}'(\mathbf{q})}} \log \left(1 + K e^{m/\tau} \frac{P(\mathbf{k}_0)}{P(\mathbf{k}_0|\mathbf{q})} \left(\mathbb{E}_{\mathbf{k}_i \sim \mathcal{D}'} \frac{P(\mathbf{k}_i|\mathbf{q})}{P(\mathbf{k}_i)} \right) \right) \\ &= \mathbb{E}_{\mathbf{q} \sim \mathcal{D}, \mathbf{k}_0 \sim \mathcal{D}'(\mathbf{q})} \log \left(1 + K e^{m/\tau} \frac{P(\mathbf{k}_0)}{P(\mathbf{k}_0|\mathbf{q})} \right) \\ &\geq \log(1 + K e^{m/\tau}) - \mathcal{I}(\mathbf{k}_0, \mathbf{q}), \end{aligned} \quad (3)$$

where $\mathcal{I}(\cdot, \cdot)$ means mutual information. The approximation in the second row is guaranteed by *Law of Large Numbers* as well as the fact $P(\mathbf{k}_i|\mathbf{q}) \approx P(\mathbf{k}_i)$ since $\mathbf{k}_i (i > 0)$ and \mathbf{q} are “almost” independent. The inequality in the last row is resulted from $P(\mathbf{k}_0|\mathbf{q}) \geq P(\mathbf{k}_0)$ as \mathbf{k}_0 and \mathbf{q} are extracted from the same instance. Therefore the lower bound of the mutual information (noted as $f_{\text{bound}}(m, K)$) between the *positive pair* $(\mathbf{k}_0, \mathbf{q})$ is:

$$\begin{aligned} \mathcal{I}(\mathbf{k}_0, \mathbf{q}) &\geq f_{\text{bound}}(m, K) \\ &\triangleq \log(1 + K e^{m/\tau}) - \mathcal{L}_{opt} \\ &\approx \log(1 + K e^{m/\tau}) - \\ &\quad \mathbb{E}_{\mathbf{q} \sim \mathcal{D}, \mathbf{k}_0 \sim \mathcal{D}'(\mathbf{q})} \log \left(1 + K e^{m/\tau} \frac{P(\mathbf{k}_0)}{P(\mathbf{k}_0|\mathbf{q})} \right). \end{aligned} \quad (4)$$

So, it is clear that \mathcal{L}_{opt} determines the lower bound of the mutual information, **which is also satisfied when $m \neq 0$** . In the case of $m = 0$, the result is consistent with that in Oord et al. (2018). Oord et al. (2018) further points out the bound increases with K , which indicates larger K

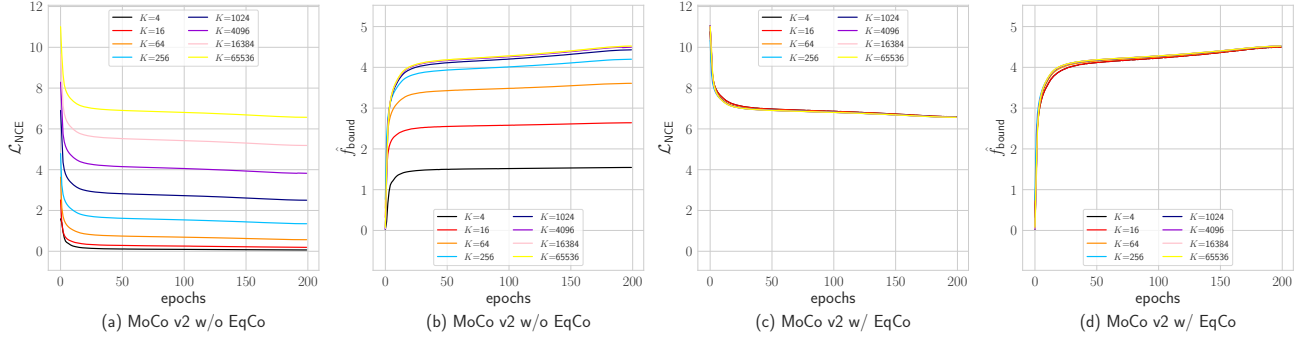


Figure 1: Evolution of the InfoNCE loss \mathcal{L}_{NCE} (Eq. 1) and *empirical mutual information lower bound* \hat{f}_{bound} during training. We use $\alpha = 65536$ for *EqCo*. Results are evaluated with *MoCo v2* on ImageNet. Refer to the discussion subsection after Proposition 1 for details. Best viewed in color.

encourages to learn more mutual information thus could help to improve the performance.

Nevertheless, different from (Oord et al., 2018) our model does not require m to be zero, so the lower bound in Eq. 4 is also a function of $e^{m/\tau}$. Thus we have the following proposition:

Proposition 1. (*EqCo for negative pairs*) The mutual information lower bound of InfoNCE loss determined by \mathcal{L}_{opt} is irrelevant to the number of negative pairs K , if

$$m = \tau \log \frac{\alpha}{K}, \quad (5)$$

where α is a constant coefficient. And in the circumstances the bound is given by:

$$\begin{aligned} f_{\text{bound}}\left(\tau \log \frac{\alpha}{K}, K\right) &\approx f_{\text{bound}}(0, \alpha) \\ &\approx \log(1 + \alpha) - \mathbb{E}_{\mathbf{q} \sim \mathcal{D}, \mathbf{k}_0 \sim \mathcal{D}'(\mathbf{q})} \log\left(1 + \alpha \frac{\mathbb{P}(\mathbf{k}_0)}{\mathbb{P}(\mathbf{k}_0|\mathbf{q})}\right), \end{aligned} \quad (6)$$

which can be immediately obtained by substituting Eq. 5 into Eq. 4. We name Eq. 5 as “*equivalent condition*”.

Proposition 1 suggests a property of *equivalency*: under the condition of Eq. 5, no matter what the number of *physical* negative pairs K is, the “optimal” target \mathcal{L}_{opt} (Eq. 3) is “equivalent” in the sense of the same mutual information lower bound. The bound is controlled by a hyper-parameter α rather than K . Eq. 6 further implies that the lower bound also correlates to the configuration of $K = \alpha$ without *margin*, which suggests we can “mimic” the InfoNCE loss’s behavior of $K = K_0$ under a different physical negative sample size K_1 , just by applying Eq. 5 with $\alpha = K_0$. It inspires us to simplify the existing state-of-the-art frameworks (e.g. MoCo (He et al., 2020)) with fewer negative samples but as accurate as the original configurations, which will be introduced next.

Remarks 1. The equivalent condition in Eq. 5 suggests the margin m is inversely correlated with K . It is intuitive, because the larger K is, the more risks of *class collision* (Arora et al., 2019) it suffers from, so we need to avoid over-penalty for negative samples near the query, thus smaller m is used; in contrast, if K is very small, we use larger m to exploit more “hard” negative samples.

Besides, recall that the *margin* term $e^{m/\tau}$ is defined as the ratio of the prior probabilities $\mathbb{P}^-/\mathbb{P}^+$ in Eq. 2. If the equivalent condition Eq. 5 satisfies, i.e., $\mathbb{P}^-/\mathbb{P}^+ = \alpha/K$, we have $\mathbb{P}^+ = 1/(1 + \alpha)$ (notice that $K\mathbb{P}^- + \mathbb{P}^+ \equiv 1$), suggesting that the prior probability of the ground truth distribution H_0 is supposed to be a constant ignoring the number of negative samples K . While in previous works (usually without the *margin* term, or $m = 0$) we have $\mathbb{P}^+ = 1/(K + 1)$. It is hard to distinguish which prior is more reasonable. However at least, we intuitively suppose keeping a constant prior for the ground truth distribution may help to keep the optimal choices of hyper-parameters steady under different K s, which is also consistent with our empirical observations.

Remarks 2. In Proposition 1, it is worth noting that K refers to the number of negative samples *per query*. In the conventional batched training scheme, negative samples for different queries could be either (fully or partially) shared or isolated, i.e., the total number of distinguishing negatives samples *per batch* could be different, which is not ruled by Proposition 1. However, we empirically find the differences in implementation do not result in much of the performance variation.

Discussion. Up to now, the *equivalent rule* (Proposition 1) is discussed in terms of the “optimal” target \mathcal{L}_{opt} , which is however intractable in practice. As mentioned in the beginning, the empirical loss \mathcal{L}_{NCE} is derived by modeling $\mathbb{P}(\mathbf{k}_i|\mathbf{q})/\mathbb{P}(\mathbf{k}_i) \propto e^{\mathbf{q}^\top \mathbf{k}_i/\tau}$ in \mathcal{L}_{opt} . Thus we expect \mathcal{L}_{NCE} would converge to \mathcal{L}_{opt} after training, and the *em-*

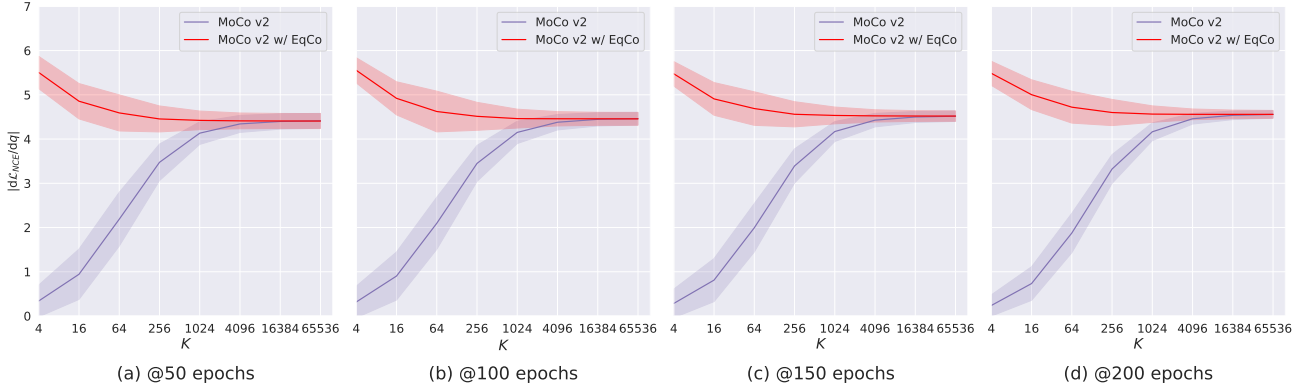


Figure 2: The means (solid line) and variances (ribbon, $\pm\sigma$) of $\|\text{d}\mathcal{L}_{NCE}/\text{d}\mathbf{q}\|$ under different K s. We train a normal MoCo v2 for 200 epochs and show the statistics at different epochs. Please refer to Theorem 2 for details. Best viewed in color.

empirical mutual information lower bound $\hat{f}_{\text{bound}}(m, K) \triangleq \log(1 + Ke^{m/\tau}) - \mathcal{L}_{NCE}$ turns out to be an estimation of the theoretical bound f_{bound} in Eq. 6. Unfortunately, we have to point that it has **NOT** been theoretically guaranteed yet: due to the complexity of neural network optimization, \mathcal{L}_{NCE} seems not necessarily to be greater than (or converge to) \mathcal{L}_{opt} . In Poole et al. (2019), for the case of $m = 0$ it can be proved that \hat{f}_{bound} indeed relates to the mutual information lower bound taking advantage of variational bounds; however, we find the approach is nontrivial to be generalized to $m \neq 0$. In addition, we run a sanity check on toy data (following Appendix B in Poole et al. (2019)) and find that occasionally even $\hat{f}_{\text{bound}} \leq \mathcal{I}(\mathbf{k}_0, \mathbf{q})$ is not satisfied when K is very small and α is large, suggesting \hat{f}_{bound} might not be a strict empirical bound. We will investigate the problem in the future.

Nevertheless, we can still experimentally evaluate how the *equivalent rule* affects \mathcal{L}_{NCE} and the empirical bound \hat{f}_{bound} in turn. In Fig. 1, we plot the evolution of \mathcal{L}_{NCE} and \hat{f}_{bound} during the training of MoCo v2 (Chen et al., 2020c) under different configurations respectively. Obviously, when it converges, without EqCo both \mathcal{L}_{NCE} and \hat{f}_{bound} keep increasing with the number of negative pairs K ; in contrast, after applying the *equivalent condition* (Eq. 5) \mathcal{L}_{NCE} and \hat{f}_{bound} converge to almost the same value under different K s respectively. The empirical results are thus consistent with Proposition 1.

The following theorem further supports the equivalent rule from backward-propagation view:

Theorem 2. Given the *equivalent condition* (Eq. 5) and a query embedding \mathbf{q} as well as the corresponding positive sample \mathbf{k}_0 , for \mathcal{L}_{NCE} in Eq. 1 the expectation of the

gradient norm w.r.t. \mathbf{q} is bounded by ²:

$$\begin{aligned} \mathbb{E}_{\mathbf{k}_i \sim \mathcal{D}'} \left\| \frac{\text{d}\mathcal{L}_{NCE}}{\text{d}\mathbf{q}} \right\| &\leq \frac{2}{\tau} \left(1 - \frac{\exp(\mathbf{q}^\top \mathbf{k}_0 / \tau)}{\exp(\mathbf{q}^\top \mathbf{k}_0 / \tau) + \alpha \mathbb{E}_{\mathbf{k}_i \sim \mathcal{D}'} [\exp(\mathbf{q}^\top \mathbf{k}_i / \tau)]} \right). \end{aligned} \quad (7)$$

Please refer to Appendix A for the detailed proof. Note that we assume the embedding vectors are *normalized*, i.e., $\|\mathbf{k}_i\| = 1 (i = 0, \dots, K)$, which is also a convention in recent contrastive learning works.

Theorem 2 indicates that, equipped with the equivalent rule (Eq. 5), the upper bound of the gradient norm is irrelevant to the number of negative samples K . Fig. 2 further validates our theory: the gradient norm becomes much more steady after using EqCo under different K s. Since the size of K affects little on the gradient magnitude, gradient scaling techniques, e.g. *linear scaling rule*, are not required specifically for different K s. Eq. 7 also implies that the *temperature* τ significantly affects the gradient norm even EqCo is applied – it is why we only recommend to modify m for equivalence (Eq. 5), though the mutual information lower bound is determined by $e^{m/\tau}$ as a whole.

2.2. The Case of Positive Pairs

In practice the InfoNCE loss (Eq. 1) is usually optimized with *batched SGD*, which can be represented as *empirical risk minimization*:

$$\mathcal{L}_{NCE}^{\text{batch}} = \frac{1}{N} \sum_{j=1}^N \mathcal{L}_{NCE}^{(j)}(\mathbf{q}_j, \mathbf{k}_{j,0}), \quad (8)$$

²Some works (e.g., He et al. (2020)) only use $\text{d}\mathcal{L}_{NCE}/\text{d}\mathbf{q}$ for optimization. In contrast, other works (e.g. Chen et al. (2020a)) also involve $\text{d}\mathcal{L}_{NCE}/\text{d}\mathbf{k}_i$, ($i = 0, \dots, K$), which we will investigate in the future.

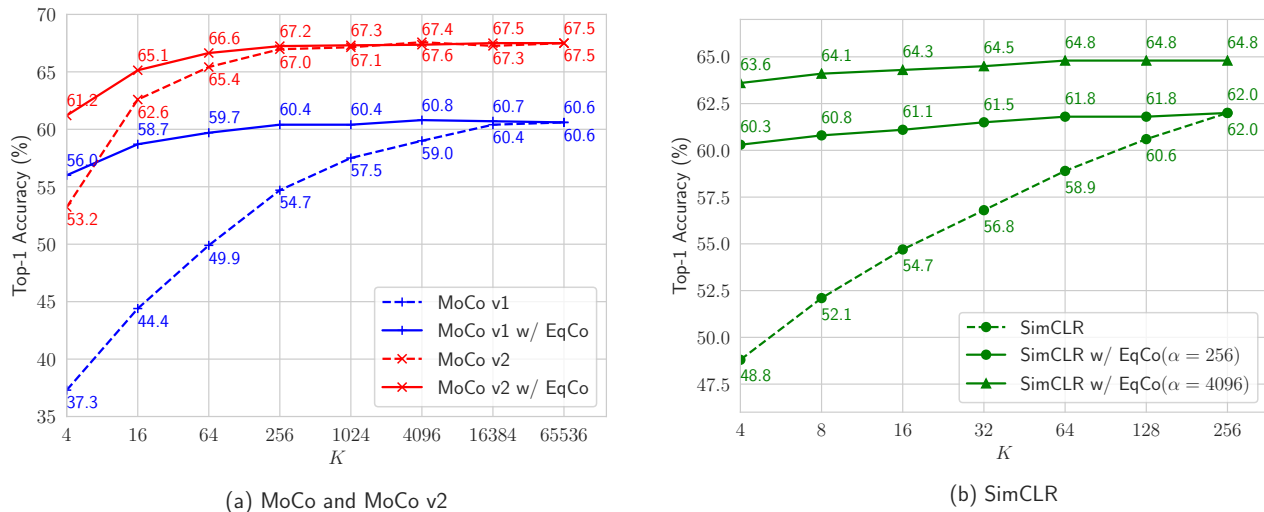


Figure 3: Comparisons with/without *EqCo* under different number of negative samples (noted by K). Results are evaluated with ImageNet top-1 accuracy using *linear evaluation protocol*. In *EqCo*, we set $\alpha = 65536$ for MoCo and MoCo v2, and $\alpha = 256$ or 4096 for SimCLR. Best viewed in color.

where N is the number of *queries* (or *positive pairs*) per batch; $(\mathbf{q}_j, \mathbf{k}_{j,0}) \sim (\mathcal{D}, \mathcal{D}'(\mathbf{q}_j))$ is the j -th positive pair, and $\mathcal{L}_{NCE}^{(j)}(\mathbf{q}_j, \mathbf{k}_{j,0})$ is the corresponding loss. For different j , $\mathcal{L}_{NCE}^{(j)}$ is (almost) independent of each other, because \mathbf{q}_j is sampled independently. Hence, Eq. 8 satisfies the form of *linear scaling rule* (Krizhevsky, 2014; Goyal et al., 2017), suggesting that **the learning rate should be adjusted proportional to the number of queries N per batch**.

Remarks 3. Previous work like *SimCLR* (Chen et al., 2020a) also proposes to apply linear scaling rule.³ The difference is, in *SimCLR* it does not clarify the concept of “batch size” refers to the number of queries or the number of keys. However in our paper, we explicitly point that the linear scaling rule needs to be applied corresponding to the number of queries per batch (N) rather than K .

2.3. Empirical Evaluation

In this subsection we conduct experiments on the three popular InfoNCE-based contrastive learning frameworks – *MoCo* (He et al., 2020), *MoCo v2* (Chen et al., 2020c) and *SimCLR* (Chen et al., 2020a) to verify our method in Sec. 2.1 and Sec. 2.2. We propose to alter K and N separately to

³In *SimCLR*, the authors find that *square-root* learning rate scaling is more desirable with *LARS* optimizer (You et al., 2017), rather than *linear scaling rule*. Also, their experiments suggest that the performance gap between large and small batch sizes become smaller under that configuration. We point that the direction is orthogonal to our equivalent rule. Besides, *SimCLR* does not explore the case of very small K s (e.g. $K \leq 128$).

examine the correctness of our *equivalent rules*.

Implementation details. We follow most of the training and evaluation settings recommended in the original papers respectively. The only difference is, for *SimCLR*, we adopt *SGD with momentum* rather than *LARS* (You et al., 2017) as the optimizer. We use *ResNet-50* (He et al., 2016) as the default network architecture. 128-d features are employed for *query* and *key* embeddings. Unless specially mentioned, all models are trained on *ImageNet* (Deng et al., 2009) for 200 epochs without using the ground truth labels. We report the top-1 accuracy under the conventional *linear evaluation protocol* according to the original paper respectively. The number of queries per batch (N) is set to 256 by default. All models are trained with 8 GPUs.

It is worth noting the way we alter the number of negative samples K independent of N during training. For MoCo and MoCo v2, we simply need to set the size of the memory bank to K . Specially, if $K < N$, in the current batch the memory bank is actually composed of K random *keys* sampled from the previous batch. While for *SimCLR*, if $K < N$ we random sample K negative keys for each query independently. We do not study the case that $K > N$ for *SimCLR*. We mainly consider the ease of implementation in designing the strategies; as mentioned in *Remarks 2* (Sec. 2.1), it does not affect the empirical conclusion.

Quantitative results. Fig. 3 illustrates the effect of our *equivalent rule* under different K s. Our experiments start with the best configurations (i.e. $K = 65536$ for MoCo

and MoCo v2, and $K = 256$ for SimCLR⁴), then we gradually reduce K and benchmark the performance. Results in Fig. 3 indicates that, without EqCo the accuracy significantly drops if K becomes very small (e.g. $K < 64$). While with EqCo, by setting α to “mimic” the optimal K , the performance surprisingly keeps steady under a wide range of K s. Fig. 3(b) further shows that in SimCLR, by setting α to a number larger than the physical batch size (e.g. 4096 vs. 256), the accuracy significantly improves from 62.0% to 64.8%,⁵ suggesting the benefit of EqCo especially when the memory is limited. The comparison fully demonstrates EqCo is essential especially when the number of negative pairs is small.

Besides, Table 1 compares the results of *MoCo* v2 under different number of queries N , while $K = 65536$ is fixed. It is clear that, with *linear scaling rule* (Krizhevsky, 2014; Goyal et al., 2017), the final performance is almost unchanged under different N , suggesting the effectiveness of our equivalent rule for N .

$N(K = 65536)$	256	512	1024
Top-1 accuracy (%)	67.5	67.5	67.4

Table 1: ImageNet accuracy (MoCo v2) vs. the number of queries per batch (N). The learning rates during training are adjusted with *linear scaling rule*.

3. SiMo: a Simpler but Stronger Baseline

EqCo inspires us to rethink the design of contrastive learning frameworks. The previous InfoNCE-based frameworks like *MoCo* and *SimCLR* heavily rely on large quantities of negative pairs to obtain high performances, hence implementation tricks such as memory bank and large batch training are introduced, which makes the system complex and tends to be costly. Thanks to EqCo, we are able to design a simpler contrastive learning framework with fewer negative pairs.

We propose *SiMo*, a simplified variant of *MoCo* v2 (Chen et al., 2020c) equipped with EqCo. We follow most of the design in Chen et al. (2020c), where the key differences are as follows:

⁴In the original paper of SimCLR (Chen et al., 2020a), the best number of negative pairs is around 4096. However, the largest K we can use in our experiment is 256 due to GPU memory limit.

⁵Our “mimicking” result (64.8%, $\alpha = 4096, K = 256$) is slightly lower than the counterpart score reported in the original SimCLR paper (66.6%, with a physical batch size of $K = 4096$), which we think may be resulted from the extra benefits of *SyncBN* along with *LARS* optimizer used in SimCLR, especially when the physical batch size is large.

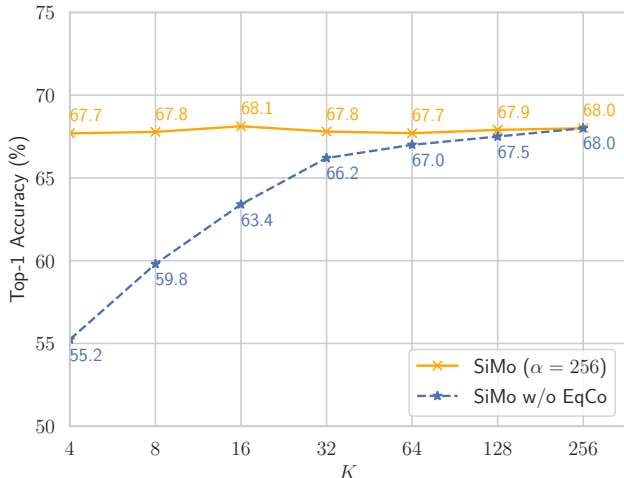


Figure 4: SiMo with/without EqCo

Method	Epochs	Top-1 (%)
CPC v2 (Hénaff et al., 2019)	200	63.8
CMC (Tian et al., 2019)	240	66.2
SimCLR (Chen et al., 2020a)	200	66.6
MoCo v2 (Chen et al., 2020c)	200	67.5
InfoMin Aug. (Tian et al., 2020)	200	70.1
SiMo ($K = 4, \alpha = 256$)	200	67.7
SiMo ($K = 16, \alpha = 256$)	200	68.1
SiMo ($K = 256, \alpha = 256$)	200	68.0
SiMo ($K = 256, \alpha = 65536$)	200	68.5
PIRL (Misra & Maaten, 2020)	800	63.6
SimCLR (Chen et al., 2020a)	1000	69.3
MoCo v2 (Chen et al., 2020c)	800	71.1
InfoMin Aug. (Tian et al., 2020)	800	73.0
SiMo ($K = 256, \alpha = 256$)	800	71.8
SiMo ($K = 256, \alpha = 65536$)	800	72.1

Table 2: State-of-the-art InfoNCE-based frameworks. Results are evaluated with ImageNet top-1 accuracy using *linear evaluation protocol*.

Memory bank. MoCo, MoCo v2 and SimCLR v2⁶ (Chen et al., 2020b) employ memory bank to maintain large number of negative embeddings \mathbf{k}_i , in which there is a side effect: every positive embedding \mathbf{k}_0 is always extracted from a “newer” network than the negatives’ in the same batch, which could harm the performance. In SiMo, we thus cancel the memory bank as we only rely on a few negative samples per batch. Instead, we use the *momentum encoder* to extract both positive and negative *key* embeddings from the current batch.

Shuffling BN vs. Sync BN. In MoCo v1/v2, shuffling BN

⁶SimCLR v2 compares the settings with/without memory bank. However, they suggest employing memory bank as the best configuration.

(He et al., 2020) is proposed to remove the obvious dissimilarities of the BN (Ioffe & Szegedy, 2015) statistics between the positive (from current mini-batch) and the negatives (from memory bank), so that the model can make predictions based on the semantic information of images rather than the BN statistics. In contrast, since the positive and negatives are from the same batch in SiMo, therefore, we use sync BN (Peng et al., 2018) for simplicity and more stable statistics. Sync BN is also used in SimCLR (Chen et al., 2020a) and SimCLR v2 (Chen et al., 2020b).

There are a few other differences, including 1) we use a BN attached to each of the fully-connected layers; 2) we introduce a warm-up stage at the beginning of the training, which follows the methodology in SimCLR (Chen et al., 2020a). Apart from all the differences mentioned above, the architecture and the training (including data augmentations) details in SiMo are *exactly* the same as MoCo v2’s. In the following text, the number of queries per batch (N) is set to 256, and the backbone network is *ResNet-50* by default.

Quantitative results. First, we empirically demonstrate the necessity of *EqCo* in SiMo framework. We choose the number of negative samples $K = 256$ as the baseline, then reduce K to evaluate the performance. Fig. 4 shows the result on ImageNet using *linear evaluation protocol*. Without EqCo, the accuracy significantly drops when K is very small. In contrast, using EqCo to “mimic” the case of large K (by setting α to 256), the accuracy almost keeps steady even under very small K s.

Table 2 further compares our SiMo with state-of-the-art self-supervised contrastive learning methods⁷ on ImageNet. Using only 4 negative samples per query, SiMo outperforms MoCo v2 whose memory bank size is 65536 (67.7% vs. 67.5%). If we increase α to 65536 to “simulate” the case under huge number of negative pairs, the accuracy further increases to 68.5%. Moreover, when we extend the training epochs to 800, we get the accuracy of 72.1%, surpassing the baseline MoCo v2 by 1.0%. The only entry that surpasses our results is *InfoMin Aug.* (Tian et al., 2020), which is mainly focuses on data generation and orthogonal to ours. The experiments indicate that SiMo is a simpler but more powerful baseline for self-supervised contrastive learning. Readers can refer to the Appendix B for more experimental results of SiMo.

4. Limitations and Future Work

In EqCo, Proposition 1 suggests that given the *equivalent condition* (Eq. 5), \mathcal{L}_{opt} under various K s are “equivalent”

⁷We mainly compare the methods with InfoNCE loss (Eq. 1) here, though recently other frameworks such as *BYOL* (Grill et al., 2020) and *SWAV* (Caron et al., 2020b) achieve better results using different loss functions.

in the sense of the same mutual information lower bound, which is also backed up with the experiments in Fig. 1. However, Fig. 3 (a) shows that if K is smaller than a certain value (e.g. $K \leq 16$), some frameworks like *MoCo v2* start to degrade significantly even with EqCo; while for other frameworks like *SimCLR* (Fig. 3 (b)) and *SiMo* (Fig. 4), the accuracy almost keeps steady for very small K s. Tschannen et al. (2019) also point that the principle of *InfoMax* cannot explain all the phenomena in contrastive learning. We will investigate the problem in the future, e.g. from other viewpoints such as gradient noise brought by small K s (Fig. 2 may give some insights).

Though the formulation of Eq. 1 is very common in the field of supervised *metric learning*, which is usually named *margin softmax cross-entropy loss* (Deng et al., 2019; Wang et al., 2018; Sun et al., 2020). Nevertheless, unfortunately, our equivalent rule seems invalid to be generalized to those problems (e.g. face recognition). The major issue lies in the approximation in Eq. 3, we need the negative samples k_i to be independent of the query q , which is not satisfied in supervised tasks.

According to Fig. 3 and Fig. 4, the benefits of EqCo become significant if K is sufficiently small (e.g. $K < 64$). But in practice, for modern computing devices (e.g. GPUs) it is not that difficult to use ~ 256 negative pairs per query. Applying EqCo to “simulate” more negative pairs via adjusting α can further boost the performance, however, whose accuracy gains become relatively marginal. For example, in Table 2 under 200 epochs training, SiMo with $\alpha = 65536$ outperforms that of $\alpha = 256$ by only 0.5%. It could be a fundamental limitation of InfoNCE loss. We will investigate the problem in the future.

References

- Arora, S., Khandeparkar, H., Khodak, M., Plevrakis, O., and Saunshi, N. A theoretical analysis of contrastive unsupervised representation learning. *arXiv preprint arXiv:1902.09229*, 2019.
- Bachman, P., Hjelm, R. D., and Buchwalter, W. Learning representations by maximizing mutual information across views. In *Advances in Neural Information Processing Systems*, pp. 15535–15545, 2019.
- Cao, Y., Xie, Z., Liu, B., Lin, Y., Zhang, Z., and Hu, H. Parametric instance classification for unsupervised visual feature learning. *arXiv preprint arXiv:2006.14618*, 2020.
- Caron, M., Misra, I., Mairal, J., Goyal, P., Bojanowski, P., and Joulin, A. Unsupervised learning of visual features by contrasting cluster assignments. *arXiv preprint arXiv:2006.09882*, 2020a.
- Caron, M., Misra, I., Mairal, J., Goyal, P., Bojanowski, P.,

- and Joulin, A. Unsupervised learning of visual features by contrasting cluster assignments. *Advances in Neural Information Processing Systems*, 33, 2020b.
- Chen, T., Kornblith, S., Norouzi, M., and Hinton, G. A simple framework for contrastive learning of visual representations. *arXiv preprint arXiv:2002.05709*, 2020a.
- Chen, T., Kornblith, S., Swersky, K., Norouzi, M., and Hinton, G. E. Big self-supervised models are strong semi-supervised learners. *Advances in Neural Information Processing Systems*, 33, 2020b.
- Chen, X. and He, K. Exploring simple siamese representation learning. *arXiv preprint arXiv:2011.10566*, 2020.
- Chen, X., Fan, H., Girshick, R., and He, K. Improved baselines with momentum contrastive learning. *arXiv preprint arXiv:2003.04297*, 2020c.
- Chuang, C.-Y., Robinson, J., Yen-Chen, L., Torralba, A., and Jegelka, S. Debaised contrastive learning. *arXiv preprint arXiv:2007.00224*, 2020.
- Deng, J., Dong, W., Socher, R., Li, L.-J., Li, K., and Fei-Fei, L. Imagenet: A large-scale hierarchical image database. In *2009 IEEE conference on computer vision and pattern recognition*, pp. 248–255. Ieee, 2009.
- Deng, J., Guo, J., Xue, N., and Zafeiriou, S. Arcface: Additive angular margin loss for deep face recognition. In *Proceedings of the IEEE Conference on Computer Vision and Pattern Recognition*, pp. 4690–4699, 2019.
- Dosovitskiy, A., Springenberg, J. T., Riedmiller, M., and Brox, T. Discriminative unsupervised feature learning with convolutional neural networks. In *Advances in neural information processing systems*, pp. 766–774, 2014.
- Ermolov, A., Siarohin, A., Sangineto, E., and Sebe, N. Whitening for self-supervised representation learning. *arXiv preprint arXiv:2007.06346*, 2020.
- Goyal, P., Dollár, P., Girshick, R., Noordhuis, P., Wesolowski, L., Kyrola, A., Tulloch, A., Jia, Y., and He, K. Accurate, large minibatch sgd: Training imagenet in 1 hour. *arXiv preprint arXiv:1706.02677*, 2017.
- Grill, J.-B., Strub, F., Althé, F., Tallec, C., Richemond, P. H., Buchatskaya, E., Doersch, C., Pires, B. A., Guo, Z. D., Azar, M. G., et al. Bootstrap your own latent: A new approach to self-supervised learning. *arXiv preprint arXiv:2006.07733*, 2020.
- Hadsell, R., Chopra, S., and LeCun, Y. Dimensionality reduction by learning an invariant mapping. In *2006 IEEE Computer Society Conference on Computer Vision and Pattern Recognition (CVPR'06)*, volume 2, pp. 1735–1742. IEEE, 2006.
- He, K., Zhang, X., Ren, S., and Sun, J. Deep residual learning for image recognition. In *Proceedings of the IEEE conference on computer vision and pattern recognition*, pp. 770–778, 2016.
- He, K., Fan, H., Wu, Y., Xie, S., and Girshick, R. Momentum contrast for unsupervised visual representation learning. In *Proceedings of the IEEE/CVF Conference on Computer Vision and Pattern Recognition*, pp. 9729–9738, 2020.
- Hénaff, O. J., Srinivas, A., De Fauw, J., Razavi, A., Doersch, C., Eslami, S., and Oord, A. v. d. Data-efficient image recognition with contrastive predictive coding. *arXiv preprint arXiv:1905.09272*, 2019.
- Ioffe, S. and Szegedy, C. Batch normalization: Accelerating deep network training by reducing internal covariate shift. *arXiv preprint arXiv:1502.03167*, 2015.
- Krizhevsky, A. One weird trick for parallelizing convolutional neural networks. *arXiv preprint arXiv:1404.5997*, 2014.
- Lin, T.-Y., Dollár, P., Girshick, R., He, K., Hariharan, B., and Belongie, S. Feature pyramid networks for object detection. In *Proceedings of the IEEE conference on computer vision and pattern recognition*, pp. 2117–2125, 2017.
- Linsker, R. Self-organization in a perceptual network. *Computer*, 21(3):105–117, 1988.
- Misra, I. and Maaten, L. v. d. Self-supervised learning of pretext-invariant representations. In *Proceedings of the IEEE/CVF Conference on Computer Vision and Pattern Recognition*, pp. 6707–6717, 2020.
- Oord, A. v. d., Li, Y., and Vinyals, O. Representation learning with contrastive predictive coding. *arXiv preprint arXiv:1807.03748*, 2018.
- Peng, C., Xiao, T., Li, Z., Jiang, Y., Zhang, X., Jia, K., Yu, G., and Sun, J. Megdet: A large mini-batch object detector. In *Proceedings of the IEEE Conference on Computer Vision and Pattern Recognition*, pp. 6181–6189, 2018.
- Poole, B., Ozair, S., Oord, A. v. d., Alemi, A. A., and Tucker, G. On variational bounds of mutual information. *arXiv preprint arXiv:1905.06922*, 2019.
- Richemond, P. H., Grill, J.-B., Althé, F., Tallec, C., Strub, F., Brock, A., Smith, S., De, S., Pascanu, R., Piot, B., et al. Byol works even without batch statistics. *arXiv preprint arXiv:2010.10241*, 2020.
- Sun, Y., Cheng, C., Zhang, Y., Zhang, C., Zheng, L., Wang, Z., and Wei, Y. Circle loss: A unified perspective of pair

- similarity optimization. In *Proceedings of the IEEE/CVF Conference on Computer Vision and Pattern Recognition*, pp. 6398–6407, 2020.
- Tian, Y., Krishnan, D., and Isola, P. Contrastive multiview coding. *arXiv preprint arXiv:1906.05849*, 2019.
- Tian, Y., Sun, C., Poole, B., Krishnan, D., Schmid, C., and Isola, P. What makes for good views for contrastive learning. *arXiv preprint arXiv:2005.10243*, 2020.
- Tschannen, M., Djolonga, J., Rubenstein, P. K., Gelly, S., and Lucic, M. On mutual information maximization for representation learning. *arXiv preprint arXiv:1907.13625*, 2019.
- Wang, H., Wang, Y., Zhou, Z., Ji, X., Gong, D., Zhou, J., Li, Z., and Liu, W. Cosface: Large margin cosine loss for deep face recognition. In *Proceedings of the IEEE Conference on Computer Vision and Pattern Recognition*, pp. 5265–5274, 2018.
- Wang, T. and Isola, P. Understanding contrastive representation learning through alignment and uniformity on the hypersphere. *arXiv preprint arXiv:2005.10242*, 2020.
- Wang, X., Zhang, H., Huang, W., and Scott, M. R. Cross-batch memory for embedding learning. In *Proceedings of the IEEE/CVF Conference on Computer Vision and Pattern Recognition*, pp. 6388–6397, 2020.
- Wu, Z., Xiong, Y., Yu, S. X., and Lin, D. Unsupervised feature learning via non-parametric instance discrimination. In *Proceedings of the IEEE Conference on Computer Vision and Pattern Recognition*, pp. 3733–3742, 2018.
- Xie, J., Zhan, X., Liu, Z., Ong, Y. S., and Loy, C. C. Delving into inter-image invariance for unsupervised visual representations. *arXiv preprint arXiv:2008.11702*, 2020.
- You, Y., Gitman, I., and Ginsburg, B. Large batch training of convolutional networks. *arXiv preprint arXiv:1708.03888*, 2017.

A. Proof of Theorem 2

Given the *equivalent condition* (Eq. 5) and a query embedding \mathbf{q} as well as the corresponding positive sample \mathbf{k}_0 , for \mathcal{L}_{NCE} in Eq. 1 the expectation of the gradient norm w.r.t. \mathbf{q} is bounded by:

$$\begin{aligned} & \mathbb{E}_{\mathbf{k}_i \sim \mathcal{D}'} \left\| \frac{d\mathcal{L}_{NCE}}{d\mathbf{q}} \right\| \\ & \leq \frac{2}{\tau} \left(1 - \frac{\exp(\mathbf{q}^\top \mathbf{k}_0 / \tau)}{\exp(\mathbf{q}^\top \mathbf{k}_0 / \tau) + \alpha \mathbb{E}_{\mathbf{k}_i \sim \mathcal{D}'} [\exp(\mathbf{q}^\top \mathbf{k}_i / \tau)]} \right). \end{aligned} \quad (9)$$

Proof. For simplicity, we denote the term $\exp(\mathbf{q}^\top \mathbf{k}_i / \tau)$ as $s_i (i = 0, \dots, K)$. Then \mathcal{L}_{NCE} can be rewritten as:

$$\mathcal{L}_{NCE} = -\log \frac{s_0}{s_0 + \frac{\alpha}{K} \sum_{i=1}^K s_i} \quad (10)$$

The gradient of \mathcal{L}_{NCE} with respect to \mathbf{q} is easily to derived:

$$\begin{aligned} \frac{d\mathcal{L}_{NCE}}{d\mathbf{q}} &= -\frac{1}{\tau} \left(1 - \frac{s_0}{s_0 + \frac{\alpha}{K} \sum_{i=1}^K s_i} \right) \mathbf{k}_0 \\ &+ \frac{\alpha}{\tau K} \sum_{i=1}^K \frac{s_0}{s_0 + \frac{\alpha}{K} \sum_{i=1}^K s_i} \mathbf{k}_i, \end{aligned} \quad (11)$$

Owing to the *Triangle Inequality* and the fact that $\mathbf{k}_i (i = 0, \dots, K)$ is normalized, the norm of gradient is bounded by:

$$\begin{aligned} \left\| \frac{d\mathcal{L}_{NCE}}{d\mathbf{q}} \right\| &\leq \left| \frac{1}{\tau} \left(1 - \frac{s_0}{s_0 + \frac{\alpha}{K} \sum_{i=1}^K s_i} \right) \right| \cdot \|\mathbf{k}_0\| \\ &+ \sum_{i=1}^K \left| \frac{\alpha}{\tau K} \frac{s_0}{s_0 + \frac{\alpha}{K} \sum_{i=1}^K s_i} \right| \cdot \|\mathbf{k}_i\| \\ &= \frac{1}{\tau} \left(1 - \frac{s_0}{s_0 + \frac{\alpha}{K} \sum_{i=1}^K s_i} \right) \\ &+ \frac{1}{\tau} \sum_{i=1}^K \frac{\frac{\alpha}{K} s_i}{s_0 + \frac{\alpha}{K} \sum_{i=1}^K s_i} \\ &= \frac{2}{\tau} \left(1 - \frac{s_0}{s_0 + \frac{\alpha}{K} \sum_{i=1}^K s_i} \right) \end{aligned} \quad (12)$$

Since the cosine similarity between \mathbf{q} and $\mathbf{k}_i (i = 1, \dots, K)$ is bounded in $[-1, 1]$, we know the expectation of $\mathbb{E}_{\mathbf{k}_i \sim \mathcal{D}'} [s_i]$ exists. According to Inequality (12) and *Jensen's Inequality*, we have:

$$\begin{aligned} & \mathbb{E}_{\mathbf{k}_i \sim \mathcal{D}'} \left[\frac{2}{\tau} \left(1 - \frac{s_0}{s_0 + \frac{\alpha}{K} \sum_{i=1}^K s_i} \right) \right] \\ &= \frac{2}{\tau} \left(1 - \mathbb{E}_{\mathbf{k}_i \sim \mathcal{D}'} \left[\frac{s_0}{s_0 + \frac{\alpha}{K} \sum_{i=1}^K s_i} \right] \right) \\ &\leq \frac{2}{\tau} \left(1 - \frac{s_0}{s_0 + \alpha \mathbb{E}_{\mathbf{k}_i \sim \mathcal{D}'} [s_i]} \right) \end{aligned} \quad (13)$$

Replacing s_i by $\exp(\mathbf{q}^\top \mathbf{k}_i / \tau)$, the proof of Theorem 2 is completed. \square

B. More Experiments on SiMo

For the following experiments of this section, we report the top-1 accuracy of SiMo on ImageNet (Deng et al., 2009) under the linear evaluation protocol. The backbone of SiMo is ResNet-50 (He et al., 2016) and we train SiMo for 200 epochs unless noted otherwise.

B.1. Ablation on Momentum Update

In MoCo (He et al., 2020) and MoCo v2 (Chen et al., 2020c), the key encoder is updated by the following rule:

$$\theta_k = \beta \theta_k + (1 - \beta) \theta_q$$

where θ_q and θ_k stand for the weights of query encoder and key encoder respectively, and β is the momentum coefficient. For SiMo, we also adopt the momentum update and use the key encoder to compute the features of positive sample and negative samples.

In Table 3, we report the results of SiMo with different momentum coefficients. The number of training epochs is set to be 100, so the top-1 accuracy of baseline ($\beta = 0.999$) drops to 64.4%. Compared to the baseline, SiMo without momentum update ($\beta = 0$) is inferior, showing the advantage of momentum update.

β	0	0.999
Accuracy (%)	62.1	64.4

Table 3: Ablation on momentum update.

B.2. Ablation on BN

Table 6 shows the performance of SiMo equipped with shuffling BN or Sync BN. Likewise, we train SiMo for 100 epochs. It is easy to check out that SiMo with shuffling BN struggles to perform well. Besides, compared to MoCo v2, SiMo with shuffling BN degrades significantly, and we

α	256	1024	4096	16384	65536	262144
Accuracy (%)	68.0	68.1	68.1	68.4	68.5	68.3

Table 4: SiMo with different α .

K	256	1024	4096	16384	65536	262144
Accuracy (%)	67.0	67.1	67.6	67.3	67.5	67.4

Table 5: MoCo v2 with different K .

	Shuffling BN	Sync BN
Accuracy (%)	58.8	64.4

Table 6: Sync BN vs. shuffling BN.

conjecture that it is because the MLP structure of SiMo is more suitable for Sync BN, rather than shuffling BN.

B.3. SiMo with Different α

As shown in Sec.2.1, α is related to the lower bound of mutual information. Table 4 reveals how accuracy of SiMo varies with the choice of α . As we increase α to 65536, the accuracy tends to improve, in accordance with the Eq.6. However, when α is too large (e.g., 262144), the performance slightly drops by 0.2%.

Similar results can be found in MoCo v2. We increase K to 262144 in MoCo v2, the accuracy also descends (in Table 5).

B.4. SiMo with Wider Models

Results using wider models are presented in Table 7. For SiMo, the performance is further boosted with wider models (more channels). For instance, SiMo with ResNet-50 (2x) and ResNet-50 (4x) outperforms the baseline (68.5%) by 2% and 3.8% respectively.

Architecture	Param. (M)	α	Top-1 (%)
ResNet-50 (2x)	94	256	70.2
ResNet-50 (2x)	94	65536	70.5
ResNet-50 (4x)	375	256	71.9
ResNet-50 (4x)	375	65536	72.3

Table 7: SiMo with wider models. All models are trained with 200 epochs.

B.5. Transfer to object detection

Setup We utilize FPN (Lin et al., 2017) with a stack of 4 3×3 convolution layers in R-CNN head to validate the effectiveness of SiMo. Following the MoCo training protocol, we fine-tune with synchronized batch-normalization (Peng

et al., 2018) across GPUs. The additional initialized layers are also equipped with BN for stable training. To effectively validate the transferability of the features, the training schedule is set to be 12 epochs (known as $1\times$), in which learning rate is initialized as 0.2 and decreased at 7 and 11 epochs with a factor of 0.1. The image scales are random sampled of [640, 800] pixels during training and fixed with 800 at inference.

Results Table 8 summarizes the fine-tuning results on COCO val2017 of different pre-training methods. Random initialization indicates training COCO from scratch, and supervised represents conventional pre-training with ImageNet labels. Compared with MoCo, SiMo achieves competitive performance without large quantities of negative pairs. It is also on a par with the supervised counterpart and significantly outperforms random initialized one.

Table 8: Object detection fine-tuned on COCO.

pre-train	AP	AP ₅₀	AP ₇₅	AP _s	AP _m	AP _l
random init	31.4	49.4	34.0	17.9	32.3	41.6
supervised	39.0	59.1	42.6	22.4	42.2	50.6
MoCo v2	39.1	59.2	42.5	23.3	42.1	50.8
SiMo	39.0	59.2	42.3	22.9	41.8	50.5